JACS
JOURNAL OF THE AMERICAN CHEMICAL SOCIETY
Article
pubs.acs.org/JACS

Does Each Atom Count in the Reactivity of Vanadia Nanoclusters?

Mei-Qi Zhang,[†,‡] Yan-Xia Zhao,*[,†] Qing-Yu Liu,[†,‡] Xiao-Na Li,[†] and Sheng-Gui He*[,†]

[†]Beijing National Laboratory for Molecular Sciences, State Key Laboratory for Structural Chemistry of Unstable and Stable Species, Institute of Chemistry, Chinese Academy of Sciences, Beijing 100190, People's Republic of China

[‡]University of Chinese Academy of Sciences, Beijing 100049, People's Republic of China

Supporting Information

ABSTRACT: Vanadium oxide cluster anions $(V_2O_5)_nV_xO_y^-$ (n = 1−31; x = 0, 1; and $x + y \leq 5$) with different oxygen deficiencies ($\Delta = 2y-1-5x$ = 0, ± 1, and ±2) have been prepared by laser ablation and reacted to abstract hydrogen atoms from alkane molecules (n-butane) in a fast flow reactor. When the cluster size n is less than 25, the Δ = 1 series [$(V_2O_5)_nO^-$ clusters] that can contain atomic oxygen radical anions ($O^{\bullet-}$) generally have much higher reactivity than the other four cluster series (Δ = −2, −1, 0, and 2), indicating that *each atom counts* in the hydrogen-atom abstraction (HAA) reactivity. Unexpectedly, all of the five cluster series have similar HAA reactivity when the cluster size is greater than 25. The critical dimension of vanadia particles separating the cluster behavior (*each atom counts*) from the bulk behavior (*each atom contributes a little part*) is thus about 1.6 nm ($\sim V_{50}O_{125}$). The strong electron−phonon coupling of the vanadia particles has been proposed to create the $O^{\bullet-}$ radicals ($V^{5+} = O^{2-}$ + heat → $V^{4+}-O^{\bullet-}$) for the n > 25 clusters with Δ = −2, −1, 0, and 2. Such a mechanism is supported by a comparative study with the scandium system [$(Sc_2O_3)_nSc_xO_y^-$ (n = 1−29; x = 0, 1; and $x + y \leq 4$)] for which the Δ = 1 series [$(Sc_2O_3)_nO^-$ clusters] always have much higher HAA reactivity than the other cluster series.

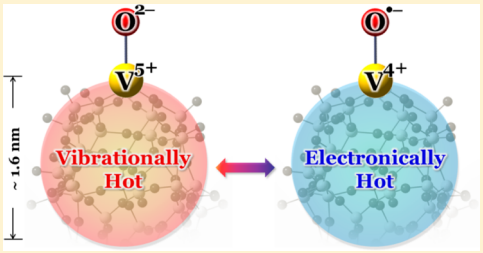

1. INTRODUCTION

Atomic clusters often have properties which vary dramatically with the addition or removal of a single atom.[1] Extensive investigations have been focused on not only uncovering the fascinating cluster behavior called "*each atom counts*"[2] but also exploring the evolution of physical and chemical properties along size atom by atom in order to understand the properties of bulk materials with a bottom-up strategy.[3] For example, the size-dependent binding energies for adsorption of CO onto Pd_n clusters show an irregular fashion for n < 100 and then increase quasi-monotonically to the bulk value, illustrating the merging of molecular orbitals to bulk electronic bands at n = 150−200.[4] In literature, the property transitions from the cluster behavior to the bulk limit have been mainly reported for elemental clusters[1,3] such as Na_n^+,[3d,5] Mg_n^-,[6] Fe_n,[7] Zn_n,[8] Ag_n^q (q = 0, ±1),[9] $Ta_n^±$ and $Ir_n^±$,[10] while such transitions have been rarely reported for composite clusters such as metal oxide clusters.[11]

Transition metal oxides (TMOs) have been widely used as catalytic materials.[12] The reactions of small- and medium-sized TMO clusters with organic and inorganic molecules have been extensively studied in order to understand elementary processes in related catalysis.[13] For example, $(Sc_2O_3)_nO^-$ (n = 1−18),[14] $(TiO_2)_nO^-$ (n = 3−25) and $(ZrO_2)_nO^-$ (n = 3−25),[15] $(CeO_2)_nO^-$ (n = 4−21),[16] $(V_2O_5)_n^+$ (n = 2−11),[17] and $(Nb_2O_5)_n^+$ (n = 1−14)[18] are reactive with reductive molecules such as alkanes and CO, whereas the clusters with more or less oxygen atoms are generally inert, indicating that the largest systems ($Sc_{36}O_{54}$, $Ti_{25}O_{50}$, $Zr_{25}O_{50}$, $Ce_{21}O_{42}$, $V_{22}O_{55}$, $Nb_{28}O_{70}$) still have the cluster behavior (*each atom counts*). It is thus very interesting to investigate the critical size at which the bulk behavior (reactivity in this study) of TMO clusters appears and the intrinsic mechanism governing the appearance, the latter of which is very important to bridge the gap between atomic clusters and bulk materials.[1,3] It is noteworthy that the previously reported TMO clusters ($M_xO_y^q$) that are reactive with alkanes and CO are usually featured with unit oxygen deficiency (Δ = 1):[19]

$$\Delta = 2y + q - mx \quad (1)$$

where m is the highest valence of M and q is the charge number. The Δ = 1 clusters such as $(Sc_2O_3)_nO^-$,[14] $(TiO_2)_nO^-$,[15] and $(V_2O_5)_nO^-$[20] usually contain atomic oxygen radical anions ($O^{\bullet-}$) that can have hydrogen-atom abstraction (HAA) reactivity with alkanes (eq 2) and oxygen-atom transfer (OAT) reactivity with CO (eq 3).[14−21]

$$O^{\bullet-} + RH \rightarrow R^{\bullet} + OH^- \quad (2)$$

$$O^{\bullet-} + CO \rightarrow CO_2 + e^- \quad (3)$$

In this study, by using a very high-resolution mass spectrometer coupled with a nanocluster source,[22] we have identified that the bulk behavior of vanadia nanoclusters appears around $V_{50}O_{125}$ which corresponds to the particle size of 1.6 nm.[23] It should be pointed out that the structures and reactivity of vanadium oxide clusters $V_xO_y^q$ (mostly x < 20) have been extensively studied[17,20,24] since the vanadium oxides are widely used materials to catalyze industrially important

Received: October 17, 2016
Published: December 12, 2016

DOI: 10.1021/jacs.6b10839
J. Am. Chem. Soc. 2017, 139, 342−347

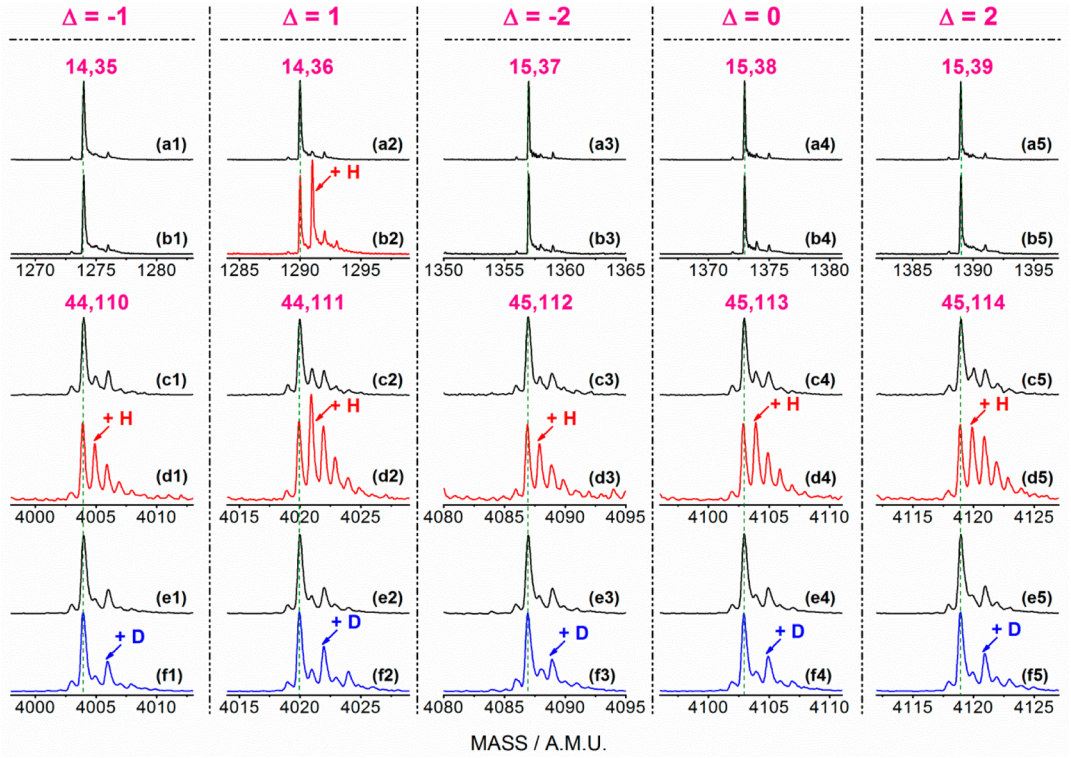

Figure 1. TOF mass spectra for the reactions of $V_xO_y^-$ (Δ = −2, −1, 0, 1, and 2) with 1.8 Pa *n*-C_4H_{10} (b), 2.0 Pa *n*-C_4H_{10} (d), and 5.0 Pa *n*-C_4D_{10} (f). Panels (a), (c), and (e) show the corresponding background spectra with Ar. The $V_xO_y^-$ are labeled as *x*,*y*. The peak heights of reactant ions were normalized.

reactions such as oxidation of SO_2 to SO_3, partial oxidation of *n*-butane to maleic anhydride, and so on.[25]

2. EXPERIMENTAL METHODS

The details of the experimental setup can be found in previous studies.[22] In brief, the vanadium oxide cluster anions ($V_xO_y^-$) were generated by laser ablation of a rotating and translating vanadium foil (99.5% purity, Alfa Aesar) in the presence of 3% O_2 seeded in a helium (99.99% purity) carrier gas with the backing pressure of about 2 atm. The clusters generated in a gas channel were expanded and reacted with *n*-C_4H_{10} (33% in He), *n*-C_4D_{10} (pure) or Ar in a fast flow reactor. After the reactions, the reactant and product ions were skimmed into the vacuum system of a tandem time-of-flight mass spectrometer (TOF-MS). After passing through two reflectors, the ions were detected by a dual microchannel plate detector. The signals from the detector were recorded with a digital oscilloscope. It should be noted that the ablation laser and oscilloscope were run at a repetition rate of 10 Hz, whereas the pulsed valves of the reactant (*n*-C_4H_{10} or *n*-C_4D_{10}) and reference (Ar) gases were operated at 5 Hz at alternate pulses for the purpose of getting better background mass spectra. The uncertainties of relative signal intensities between a pair of spectra were within 5%. For comparison, the experiments on the reactivity of scandium oxide cluster anions ($Sc_xO_y^-$) have also been conducted under similar reaction conditions.

3. RESULTS AND DISCUSSION

Size-Dependent Reactivity. The laser-ablation-generated $V_xO_y^-$ clusters can be classified into different series by their oxygen deficiencies (eq 1): Δ = −2 [$(V_2O_5)_nVO_2^-$, *n* = 6-31], Δ = −1 [$(V_2O_5)_n^-$, *n* = 2−31], Δ = 0 [$(V_2O_5)_nVO_3^-$, *n* = 1−31], Δ = 1 [$(V_2O_5)_nO^-$, *n* = 2−31], and Δ = 2 [$(V_2O_5)_nVO_4^-$, *n* = 1−31]. Typical TOF mass spectra for the reactions of Δ = −2, −1, 0, 1, and 2 clusters with *n*-C_4H_{10} and *n*-C_4D_{10} are shown in Figure 1 and Figures S1 and S2 (see Supporting Information). For small-sized clusters $V_{14,15}O_y^-$ (Figure 1b), no product signal appeared upon interaction with *n*-C_4H_{10}, except for $V_{14}O_{36}^-$ (Δ = 1) whose HAA product $V_{14}O_{36}H^-$ was generated apparently (Figure 1b2, eq 4). In sharp contrast, large-sized clusters with an additional unit of $(V_2O_5)_{15}$ ($V_{44,45}O_y^-$ in Figure 1d) all have the HAA reactivity with *n*-C_4H_{10} (eq 4), which was confirmed by isotopic labeling experiments (Figure 1f).

$$V_xO_y^- + n\text{-}C_4H_{10} \rightarrow V_xO_yH^- + C_4H_9 \quad (4)$$

In addition, the adsorption channels (Figure S3) and the double HAA channels (Figures 1d2 and 1f2) have also been observed and contribute to the overall rates of reactions. Nevertheless, the overall reactivity is mainly ascribed to the HAA reactions ($V_xO_yH_{1,2}^-$). For example, the branching ratios of HAA channels for $V_{44}O_{111}^-$ and $V_{45}O_{113}^-$ in Figure 1d are estimated to be 70.5% and 81.7%, respectively.

The pseudo-first-order rate constant (k_1)[26] for the reaction between each of the clusters and *n*-C_4H_{10} is determined (see Figure S4 for one example) and the reaction efficiency (Φ) could be calculated by using the following equation:

$$\Phi = k_1/k_{collision} \quad (5)$$

in which $k_{collision}$ is the collisional rate constant calculated by using the hard sphere average dipole orientation theory (Figure S5).[27] Figure 2 plots the relative efficiencies Φ^{rel} [= $\Phi(V_xO_y^- + n\text{-}C_4H_{10})/\Phi(V_{14}O_{36}^- + n\text{-}C_4H_{10})$] of the overall reaction for Δ = −2, −1, 0, 1, and 2 cluster series. Note that the HAA channel accounts to more than 65% of the overall reaction (Figure S3). The size-dependency of the reactivity for the Δ = 1 and Δ ≠ 1 clusters differs a lot. The $(V_2O_5)_nO^-$ (Δ = 1) clusters show a sharp reactivity increase as the cluster size increases and a local

DOI: 10.1021/jacs.6b10839
J. Am. Chem. Soc. 2017, 139, 342−347

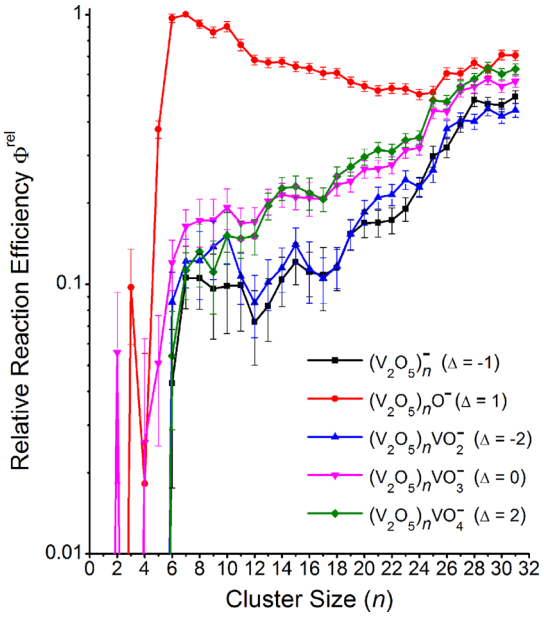

Figure 2. Relative reaction efficiencies (Φ^{rel}) of $V_xO_y^-$ ($\Delta = -2, -1, 0, 1$, and 2) with n-C_4H_{10}. The Φ^{rel} values are relative to the absolute reaction efficiency $\Phi(V_{14}O_{36}^- + n\text{-}C_4H_{10}) = 0.021 \pm 0.004$. The y-axis is unitless.

maximum appears at $n = 7$. As the cluster size further increases, the reaction efficiency decreases slightly and is nearly constant for $n > 25$. In sharp contrast, the reaction efficiencies of the other four cluster series with $\Delta = -2, -1, 0$, and 2 generally increase monotonically when the clusters are upsized and the reaction efficiencies of the $n > 25$ clusters are more than 1 order of magnitude larger than those of the small ones ($n = 1$–6). Finally, for $n > 25$ (~1.6 nm),[23] the relative reaction efficiencies of $V_xO_y^-$ clusters with different oxygen deficiencies ($\Delta = 1$ and $\Delta \neq 1$) are very close to each other (within a factor of 1.9), which indicates the appearance of the bulk behavior in the reaction with n-butane (mainly HAA reactivity).

Reactivity Origin of the $\Delta \neq 1$ Clusters. Extensive investigations on small- and medium-sized $M_xO_y^q$ systems have revealed that TMO clusters possessing the $O^{\bullet-}$ radicals could react with various small molecules[14−21] under thermal collision conditions, whereas the $O^{\bullet-}$ free TMO clusters are generally inert under similar conditions.[14−20,21d] Recently, studies on TMO clusters with dimensions up to nanosize have confirmed both experimentally and theoretically that nanosized clusters with $\Delta = 1$, which can contain the reactive $O^{\bullet-}$ species, show unique reactivity compared to the $\Delta \neq 1$ clusters that usually have no $O^{\bullet-}$ centers.[14−18,21d] The observed reactivity of the $V_xO_y^-$ clusters with $\Delta = -2, -1, 0$, and 2 herein is thus unexpected.

Nanoclusters possess substantial intracluster vibrational energy (E_{vib}), which can be estimated as $E_{vib} \approx sk_BT$ (s is the vibrational degree of freedom, k_B is the Boltzmann constant, T is the temperature of the cluster). The E_{vib} scales linearly with the cluster size. For example, at $T = 300$ K the E_{vib} value of $(V_2O_5)_nVO_3^-$ ($\Delta = 0$) increases from 1.24 eV at $n = 2$ to 16.4 eV at $n = 30$. The high E_{vib} of the large clusters may be used directly to induce the reactions with n-butane. The encounter complex of $V_xO_y^-$ and n-C_4H_{10} carries excess energy ($E_{exc} = E_k + E_{vib}$), in which E_k is the center-of-mass collisional energy and $E_k = 1/2\ \mu v^2$ (μ is the reduced mass of the cluster with n-C_4H_{10} and $v \approx 600$ m/s). The Rice−Ramsperger−Kassel−Marcus (RRKM) theory can be adopted to estimate the rate to abstract a hydrogen atom from an n-butane molecule:[28]

$$k_{RRKM} = \frac{k_BT}{h}\left(1 - \frac{E_a}{E_{vib} + E_k}\right)^{s-1} \quad (6)$$

where h is the Plank constant and E_a is the reaction barrier, which is around 1.5 eV from the quantum chemistry calculations on the HAA process mediated with the O^{2-} species in the ground state of $V_5O_{13}^-$ (Figure S6 in Supporting Information). The temperature of the laser-ablation-generated clusters could be in the range of 300−700 K.[29] With eq 6, the rates to abstract a hydrogen atom from n-C_4H_{10} by $(V_2O_5)_{30}VO_3^-$ are 4×10^{-14} s^{-1} and 2×10^2 s^{-1} for $T =$ 300 and 700 K, respectively. These rates are too slow so that the HAA reactivity of the $\Delta \neq 1$ clusters (with high HAA barriers around 1.5 eV) could not be observed by the experiments.

The previous studies have indicated that the HAA process mediated with the $O^{\bullet-}$ species on $\Delta = 1$ TMO clusters usually has negligible or very small reaction barriers.[14,17−19,21b−d] Thus, we speculate that those $V_xO_y^-$ clusters with obvious $V_xO_yH^-$ products formation in the reactions with n-C_4H_{10} should also possess $O^{\bullet-}$ units. The electronically ground state of the $\Delta = 1$ $V_xO_y^-$ clusters already has the $O^{\bullet-}$ species,[14−19,21d] while for the clusters with $\Delta = -2, -1, 0$, or 2, the electronic excitation is required. For condensed-phase systems, it has been proposed that $O^{\bullet-}$ may be generated spontaneously by an electron transfer from the oxygen anion O^{2-} to the metal cation M^{n+} at sufficiently high temperatures:[30]

$$M^{n+}{=}O^{2-} + \text{heat} \rightarrow M^{(n-1)+}{-}O^{\bullet-} \quad (7)$$

This mechanism for bulk systems may function for nanosized $V_xO_y^-$ clusters to generate the $O^{\bullet-}$ radicals:

$$V^{5+}{=}O^{2-} + E_{vib} \rightarrow V^{4+}{-}O^{\bullet-} \quad (8)$$

The mechanism (8) rationalizes the reactivity origin of large $\Delta \neq 1$ clusters that have high vibrational energy E_{vib}. For small clusters, the E_{vib} is small and thus the $\Delta \neq 1$ clusters are nearly inert in the HAA reaction (Figure 1).

In addition to enough intracluster vibrational energy, sufficient electron−phonon coupling is also required so that the electron transfer process (eq 8) can occur. Strong electron−phonon coupling has been identified for many vanadia based systems, such as pure[31] or doped V_2O_5 single crystals,[32] semiconducting V_2O_5 gels,[33] oxide glasses with V_2O_5,[34] pure[35] or doped VO_2.[36] Moreover, due to quantum-size effect, the electron−phonon coupling can be enhanced in isolated (gas-phase) nanoclusters of which the atoms are in confined space.[37] Therefore, we propose that strong electron−phonon coupling and the high vibrational energy in large $V_xO_y^-$ ($x \geq 50$) clusters lead to the generation of the reactive $O^{\bullet-}$ radicals through eq 8. Such generated $O^{\bullet-}$ radicals are responsible for the observed HAA reactivity (reactions 2 and 4) of the large $\Delta \neq 1$ clusters (Figure 1).

Similar reactivity has also been observed for photochemically excited vanadium oxide clusters in condensed phase.[38] For example, it has been reported that for two halide-templated bismuth vanadium oxide clusters, the irradiation into a ligand-to-metal charge-transfer band results in the formation of catalytically active state, i.e., triplet state.[39] Herein, the active states for $(V_2O_5)_nVO_3^-$ clusters with $\Delta = 0$ may also be of triplet multiplicity. In order to verify the formation of atomic

DOI: 10.1021/jacs.6b10839
J. Am. Chem. Soc. 2017, 139, 342−347

oxygen radicals in the excited states, density functional theory (DFT) calculations have been performed to study the structural properties of $(V_2O_5)_{1-5}VO_3^-$ clusters using the hybrid B3LYP functional (see Supporting Information for computational details). These calculations have confirmed that by transferring an electron from oxygen anions to vanadium cations, the generated triplet state contains atomic oxygen radicals (Figure S7).

Comparison with Scandia Clusters. To further support the aforementioned mechanism, the HAA reactivity of the scandia cluster anions $[(Sc_2O_3)_nSc_xO_y^-$, $n \leq 29$ and $x = 0, 1$; $\Delta = 2y - 1 - 3x = 0, \pm 1$, and $\pm 2]$ has also been studied. Typical mass spectra and the size-dependent relative reaction efficiencies Φ^{rel} $[= \Phi(Sc_xO_y^- + n\text{-}C_4H_{10})/\Phi(Sc_{36}O_{55}^- + n\text{-}C_4H_{10})$, in which the Φ values were calculated by using eq 5$]$[40] are shown in Figures S8 and 3, respectively. The $(Sc_2O_3)_nO^-$ clusters with $\Delta = 1$ are highly reactive toward n-C_4H_{10}, and the HAA reactivity generally increases as the cluster size increases (Figure 3). The cluster series with other oxygen deficiencies such as $\Delta = 0$ and 2 do not react or react very slowly with n-C_4H_{10} even at high n-C_4H_{10} pressures in the studied size range. As a result, *each atom still counts* for the HAA reactivity of the scandium oxide clusters as large as $Sc_{52}O_y^-$. In sharp contrast, the bulk behavior was identified for the vanadium oxide clusters starting from around $V_{50}O_y^-$.

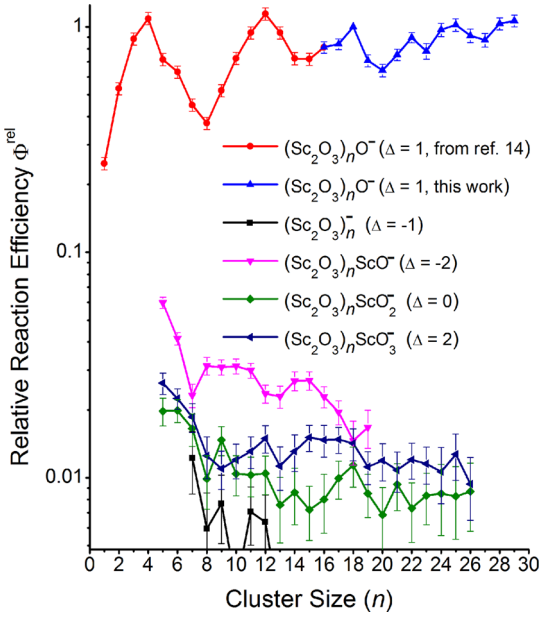

Figure 3. Relative reaction efficiencies (Φ^{rel}) of $Sc_xO_y^-$ ($\Delta = -2, -1$, 0, 1, and 2) with n-C_4H_{10}. The Φ^{rel} values are relative to the absolute reaction efficiency $\Phi(Sc_{36}O_{55}^- + n\text{-}C_4H_{10}) = 0.246 \pm 0.056$. The y-axis is unitless.

The experiments indicated that $Sc_xO_y^-$ clusters behave quite differently from $V_xO_y^-$ clusters in the HAA reactions. Three factors may be responsible for the unobserved or very low reactivity of large $Sc_xO_y^-$ ($x \geq 50$) clusters with $\Delta \neq 1$: (1) the electronegativity difference between Sc atom (1.36) and O atom (3.44) is larger than that between V atom (1.63) and O atom,[41] so the thermal electron transfer from O^{2-} to Sc^{3+} is more difficult than that from O^{2-} to V^{5+}; (2) bulk V_2O_5 is a semiconductor with an energy gap (E_g) of 2.3 eV between the valence band (VB) and the conduction band (CB)[42] while bulk Sc_2O_3 is an insulator with a band gap of 6.0 eV;[43] and (3) the electron–phonon coupling effect in scandia system can be less efficient than that in vanadia system. As a result, it is more difficult to transfer an electron from the O-based orbitals to the Sc-based orbitals than to the V-based orbitals, as shown in Figure 4a. In order to get some semiquantitative insights into the energy gaps of nanoclusters, we performed DFT calculations on two prototype clusters ($V_{11}O_{28}^-$ and $Sc_{11}O_{17}^-$ anions). As illustrated in Figure 4b, the energy of electron excitation from singlet state to triplet state for the most stable structure of $V_{11}O_{28}^-$ is 1.86 eV, while the value (3.59 eV) for $Sc_{11}O_{17}^-$ is larger by a factor of about 2. The comparative study suggests that for the investigated large $M_xO_y^-$ (M = Sc and V, $x \geq 50$) clusters, the electron–phonon coupling generates the $O^{\bullet-}$ radicals for vanadium rather than the scandium system.

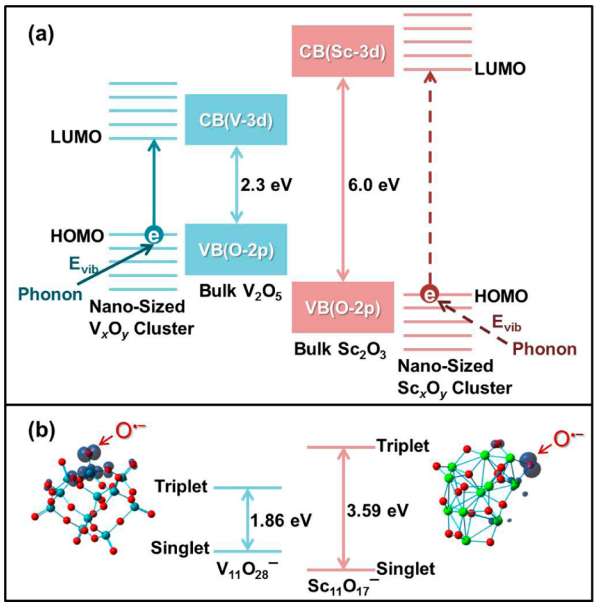

Figure 4. (a) Schematic description of thermal electron transfer processes in vanadia and scandia systems. The HOMO and the LUMO denote the highest occupied molecular orbital and the lowest unoccupied molecular orbital of the nanosized clusters, respectively. (b) Energy gaps between singlet states and corresponding triplet states for the most stable structures of $V_{11}O_{28}^-$ and $Sc_{11}O_{17}^-$ anions calculated at B3LYP/TZVP level. Spin density isosurfaces for the triplet states are also plotted. Color scheme: V, blue; Sc, green; O, red.

The mechanism of $O^{\bullet-}$ generation in vanadium system turns out to be the fundamental basis to observe the bulk behavior of the large $V_xO_y^-$ ($x \geq 50$) clusters. In these large and nanosized $V_xO_y^-$ clusters, "*each atom counts*" does not work in the HAA reactivity. In constrast, *each atom contributes a little part* ($3k_BT$) to the vibrational energy which can be sufficiently high so that the electron transfer (eq 8) can occur. Such a mechanism can lead to a dramatic reactivity enhancement for isolated (gas-phase) oxide nanoparticles. It is noteworthy that for supported or assembled oxide nanoparticles, the quantum-size effect and the electron–phonon coupling may not be as strong as in the isolated nanoparticles. It would be interesting to compare the reactivity of vanadium nanoparticles in gas-phase and condensed-phase systems in future.

DOI: 10.1021/jacs.6b10839
J. Am. Chem. Soc. 2017, 139, 342–347

4. CONCLUSION

In summary, the size-dependent hydrogen-atom abstraction reactivity of vanadium oxide cluster anions $(V_2O_5)_nV_{0,1}O_{0-4}^-$ (n = 1−31) with different oxygen deficiencies (Δ = −2, −1, 0, 1, and 2) has been investigated by using high-resolution mass spectrometry. The cluster behavior (*each atom counts*) in the reactivity was observed for small clusters. For large clusters starting from around $V_{50}O_y^-$, all of the clusters have similar reactivity so the bulk behavior (*each atom contributes a little part*) of the reactivity has been identified. This study proposed that in these large vanadium oxide particles, *each atom contributes a little part* to the vibrational energy that can be sufficiently high to transfer electrons from oxygen anions to vanadium cations to form the reactive oxygen radicals (V^{5+}═O^{2-} + E_{vib} → V^{4+}−$O^{\bullet-}$) through electron−phonon coupling. The generation of $O^{\bullet-}$ can dramatically enhance the reactivity of isolated (gas-phase) oxide nanoparticles. This mechanism has been further supported by a comparative study on scandium oxide clusters $Sc_xO_y^-$, which showed cluster behavior (*each atom counts*) for systems as large as $Sc_{52}O_y^-$.

■ ASSOCIATED CONTENT

Supporting Information

The Supporting Information is available free of charge on the ACS Publications website at DOI: 10.1021/jacs.6b10839.

Figures S1−S9 giving additional experimental and computational results, details of the theoretical and experimental rate constants, and details of computational methods (PDF)

■ AUTHOR INFORMATION

Corresponding Authors

*chemzyx@iccas.ac.cn

*shengguihe@iccas.ac.cn

ORCID

Sheng-Gui He: 0000-0002-9919-6909

Notes

The authors declare no competing financial interest.

■ ACKNOWLEDGMENTS

This work was supported by the National Natural Science Foundation of China (Nos. 21325314, 21273247, and 21573247), the Major Research Plan of China (No. 2013-CB834603), and the Chinese Academy of Sciences (YZ201318 and XDA09030101).

■ REFERENCES

(1) *Clusters of Atoms and Molecules: Theory, Experiment, and Clusters of Atoms*; Haberland, H., Ed.; Springer-Verlag: Berlin/Heidelberg, 1994.

(2) (a) Baletto, F.; Ferrando, R. *Rev. Mod. Phys.* **2005**, *77*, 371. (b) Ferrando, R.; Jellinek, J.; Johnston, R. L. *Chem. Rev.* **2008**, *108*, 845. (c) Wang, L. M.; Wang, L. S. *Nanoscale* **2012**, *4*, 4038. (d) Young, R. M.; Neumark, D. M. *Chem. Rev.* **2012**, *112*, 5553. (e) Schlangen, M.; Schwarz, H. *Catal. Lett.* **2012**, *142*, 1265. (f) Tyo, E. C.; Vajda, S. *Nat. Nanotechnol.* **2015**, *10*, 577.

(3) (a) *Physics and Chemistry of Finite Systems: From Clusters to Crystals*; Jena, P., Khanna, S. N., Rao, B. K., Eds.; Springer: Netherlands, 1992. (b) de Heer, W. A. *Rev. Mod. Phys.* **1993**, *65*, 611. (c) Castleman, A. W.; Bowen, K. H. *J. Phys. Chem.* **1996**, *100*, 12911. (d) Aguado, A.; Jarrold, M. F. *Annu. Rev. Phys. Chem.* **2011**, *62*, 151. (e) Zhao, J. J.; Huang, X. M.; Jin, P.; Chen, Z. F. *Coord. Chem. Rev.* **2015**, *289*, 315.

(4) Sitja, G.; Moal, S. L.; Marsault, M.; Hamm, G.; Leroy, F.; Henry, C. R. *Nano Lett.* **2013**, *13*, 1977.

(5) (a) Haberland, H.; Hippler, T.; Donges, J.; Kostko, O.; Schmidt, M.; von Issendorff, B. *Phys. Rev. Lett.* **2005**, *94*, 035701. (b) Maier, M.; Wrigge, G.; Hoffmann, M. A.; Didier, P.; von Issendorff, B. *Phys. Rev. Lett.* **2006**, *96*, 117405.

(6) Thomas, O. C.; Zheng, W. J.; Xu, S. J.; Bowen, K. H. *Phys. Rev. Lett.* **2002**, *89*, 213403.

(7) Billas, I. M. L.; Becker, J. A.; Châtelain, A.; de Heer, W. A. *Phys. Rev. Lett.* **1993**, *71*, 4067.

(8) Aguado, A.; Vega, A.; Lebon, A.; von Issendorff, B. *Angew. Chem., Int. Ed.* **2015**, *54*, 2111.

(9) (a) Chakraborty, I.; Erusappan, J.; Govindarajan, A.; Sugi, K. S.; Udayabhaskararao, T.; Ghosh, A.; Pradeep, T. *Nanoscale* **2014**, *6*, 8024. (b) Ma, J.; Cao, X. Z.; Liu, H.; Yin, B. Q.; Xing, X. P. *Phys. Chem. Chem. Phys.* **2016**, *18*, 12819.

(10) Balteanu, I.; Achatz, U.; Balaj, O. P.; Fox, B. S.; Beyer, M. K.; Bondybey, V. E. *Int. J. Mass Spectrom.* **2003**, *229*, 61.

(11) (a) Zhai, H. J.; Wang, L. S. *J. Am. Chem. Soc.* **2007**, *129*, 3022. (b) Demyk, K.; van Heijnsbergen, D.; von Helden, G.; Meijer, G. *Astron. Astrophys.* **2004**, *420*, 547.

(12) (a) Hodnett, B. K. *Heterogeneous Catalytic Oxidation*; John Wiley & Sons: New York, 2000. (b) Rase, H. F. *Handbook of Commercial Catalysts: Heterogeneous Catalysts*; CRC Press: Boca Raton, FL, 2000. (c) Centi, G.; Cavani, F.; Trifirò, F. *Selective Oxidation by Heterogeneous Catalysis*; Kluwer Academic/Plenum Publishers: New York, 2001. (d) *Metal Oxides: Chemistry and Applications*; Fierro, J. L. G., Ed.; Taylor & Francis: New York, 2006. (e) Lloyd, L. *Handbook of Industrial Catalysis*; Springer: New York, 2011.

(13) (a) Böhme, D. K.; Schwarz, H. *Angew. Chem., Int. Ed.* **2005**, *44*, 2336. (b) Gong, Y.; Zhou, M. F.; Andrews, L. *Chem. Rev.* **2009**, *109*, 6765. (c) Roithová, J.; Schröder, D. *Chem. Rev.* **2010**, *110*, 1170. (d) Zhai, H. J.; Wang, L. S. *Chem. Phys. Lett.* **2010**, *500*, 185. (e) Castleman, A. W. *Catal. Lett.* **2011**, *141*, 1243. (f) Yin, S.; Bernstein, E. R. *Int. J. Mass Spectrom.* **2012**, *321*, 49. (g) Lang, S. M.; Bernhardt, T. M. *Phys. Chem. Chem. Phys.* **2012**, *14*, 9255. (h) Asmis, K. R. *Phys. Chem. Chem. Phys.* **2012**, *14*, 9270. (i) O'Hair, R. A. J. *Int. J. Mass Spectrom.* **2015**, *377*, 121. (j) Schwarz, H. *Angew. Chem., Int. Ed.* **2015**, *54*, 10090. (k) Zhao, Y. X.; Liu, Q. Y.; Zhang, M. Q.; He, S. G. *Dalton Trans.* **2016**, *45*, 11471.

(14) Tian, L. H.; Meng, J. H.; Wu, X. N.; Zhao, Y. X.; Ding, X. L.; He, S. G.; Ma, T. M. *Chem. - Eur. J.* **2014**, *20*, 1167.

(15) Ma, J. B.; Xu, B.; Meng, J. H.; Wu, X. N.; Ding, X. L.; Li, X. N.; He, S. G. *J. Am. Chem. Soc.* **2013**, *135*, 2991.

(16) Wu, X. N.; Ding, X. L.; Bai, S. M.; Xu, B.; He, S. G.; Shi, Q. *J. Phys. Chem. C* **2011**, *115*, 13329.

(17) Wu, X. N.; Ding, X. L.; Li, Z. Y.; Zhao, Y. X.; He, S. G. *J. Phys. Chem. C* **2014**, *118*, 24062.

(18) Ding, X. L.; Wang, D.; Wu, X. N.; Li, Z. Y.; Zhao, Y. X.; He, S. G. *J. Chem. Phys.* **2015**, *143*, 124312.

(19) (a) Zhao, Y. X.; Wu, X. N.; Ma, J. B.; He, S. G.; Ding, X. L. *Phys. Chem. Chem. Phys.* **2011**, *13*, 1925. (b) Ding, X. L.; Wu, X. N.; Zhao, Y. X.; He, S. G. *Acc. Chem. Res.* **2012**, *45*, 382.

(20) Yuan, Z.; Li, Z. Y.; Zhou, Z. X.; Liu, Q. Y.; Zhao, Y. X.; He, S. G. *J. Phys. Chem. C* **2014**, *118*, 14967.

(21) (a) Nößler, M.; Mitrić, R.; Bonačić-Koutecký, V.; Johnson, G. E.; Tyo, E. C.; Castleman, A. W. *Angew. Chem., Int. Ed.* **2010**, *49*, 407. (b) Schwarz, H. *Chem. Phys. Lett.* **2015**, *629*, 91. (c) Dietl, N.; Schlangen, M.; Schwarz, H. *Angew. Chem., Int. Ed.* **2012**, *51*, 5544. (d) Wu, X. N.; Xu, B.; Meng, J. H.; He, S. G. *Int. J. Mass Spectrom.* **2012**, *310*, 57.

(22) (a) Yuan, Z.; Liu, Q. Y.; Li, X. N.; He, S. G. *Int. J. Mass Spectrom.* **2016**, *407*, 62. (b) Liu, Q. Y.; Yuan, Z.; Zhao, Y. X.; He, S. G. *J. Phys. Chem. C* **2016**, *120*, 17081.

(23) The diameters of $V_xO_y^-$ clusters were estimated for a round ball with the mass density of the bulk V_2O_5 materials (3.357 g cm^{-3}).

DOI: 10.1021/jacs.6b10839
J. Am. Chem. Soc. 2017, 139, 342−347

(24) (a) Fielicke, A.; Rademann, K. *Phys. Chem. Chem. Phys.* **2002**, *4*, 2621. (b) Justes, D. R.; Mitrić, R.; Moore, N. A.; Bonačić-Koutecký, V.; Castleman, A. W. *J. Am. Chem. Soc.* **2003**, *125*, 6289. (c) Feyel, S.; Schröder, D.; Rozanska, X.; Sauer, J.; Schwarz, H. *Angew. Chem., Int. Ed.* **2006**, *45*, 4677. (d) Feyel, S.; Döbler, J.; Schröder, D.; Sauer, J.; Schwarz, H. *Angew. Chem., Int. Ed.* **2006**, *45*, 4681. (e) Asmis, K. R.; Sauer, J. *Mass Spectrom. Rev.* **2007**, *26*, 542. (f) Zhai, H. J.; Döbler, J.; Sauer, J.; Wang, L. S. *J. Am. Chem. Soc.* **2007**, *129*, 13270. (g) Li, S. H.; Mirabal, A.; Demuth, J.; Wöste, L.; Siebert, T. *J. Am. Chem. Soc.* **2008**, *130*, 16832. (h) Dong, F.; Heinbuch, S.; Xie, Y.; Bernstein, E. R.; Rocca, J. J.; Wang, Z. C.; Ding, X. L.; He, S. G. *J. Am. Chem. Soc.* **2009**, *131*, 1057. (i) Zhao, Y. X.; Wu, X. N.; Wang, Z. C.; He, S. G.; Ding, X. L. *Chem. Commun.* **2010**, *46*, 1736. (j) Zhou, M. F.; Wang, C. X.; Zhuang, J.; Zhao, Y. Y.; Zheng, X. M. *J. Phys. Chem. A* **2011**, *115*, 39. (k) Wu, J. W. J.; Moriyama, R.; Tahara, H.; Ohshimo, K.; Misaizu, F. *J. Phys. Chem. A* **2016**, *120*, 3788. (l) Kurokawa, H.; Mafuné, F. *Chem. Phys. Lett.* **2016**, *651*, 24.

(25) (a) Centi, G.; Trifirò, F.; Ebner, J. R.; Franchetti, V. M. *Chem. Rev.* **1988**, *88*, 55. (b) Dunn, J. P.; Stenger, H. G.; Wachs, I. E. *Catal. Today* **1999**, *51*, 301. (c) Weckhuysen, B. M.; Keller, D. E. *Catal. Today* **2003**, *78*, 25. (d) Zhang, X.; Tang, Y. Y.; Qu, S. Q.; Da, J. W.; Hao, Z. P. *ACS Catal.* **2015**, *5*, 1053. (e) Artiglia, L.; Agnoli, S.; Granozzi, G. *Coord. Chem. Rev.* **2015**, *301*, 106.

(26) (a) The pseudo-first-order rate constant k_1 for a reaction in the fast flow reactor can be estimated by using the equation $k_1 = \ln(I_T/I_R)/(\rho t_R)$, in which I_T is the total ion intensity including product ion contribution; I_R is the intensity of the reactant cluster ions after the reaction; ρ is the molecular density of the reactant; and t_R is the reaction time in the reactor. The relative rate constants k_1^{rel} $[=k_1(V_xO_y^- + n\text{-}C_4H_{10})/k_1(V_{14}O_{36}^- + n\text{-}C_4H_{10})]$ are independent of ρ and t_R. The accurate absolute rate constant $k_1(V_{14}O_{36}^- + n\text{-}C_4H_{10})$ was fitted to be 2.19×10^{-11} cm^3 molecule^{-1} s^{-1} from a pressure-dependent experiment. Note that for single and double HAA, the contributions of isotopic peaks (^{17}O and ^{18}O) and reactions with residual water in the gas handling system in the reference spectra have been subtracted from the intensities of the reaction products with *n*-butane. (b) Xue, W.; Wang, Z. C.; He, S. G.; Xie, Y.; Bernstein, E. R. *J. Am. Chem. Soc.* **2008**, *130*, 15879.

(27) Kummerlöwe, G.; Beyer, M. K. *Int. J. Mass Spectrom.* **2005**, *244*, 84.

(28) Steinfeld, J. I.; Francisco, J. S.; Hase, W. L.*Chemical Kinetics and Dynamics*; Prentice-Hall: Upper Saddle River, NJ, 1999; p 231.

(29) Matsuda, Y.; Bernstein, E. R. *J. Phys. Chem. A* **2005**, *109*, 3803.

(30) Yang, T. J.; Lunsford, J. H. *J. Catal.* **1980**, *63*, 505.

(31) Ioffe, V. A.; Patrina, I. B. *Phys. Status Solidi B* **1970**, *40*, 389.

(32) Presura, C.; Popinciuc, M.; van Loosdrecht, P. H. M.; van der Marel, D.; Mostovoy, M.; Yamauchi, T.; Ueda, Y. *Phys. Rev. Lett.* **2003**, *90*, 026402.

(33) Sanchez, C.; Babonneau, F.; Morineau, R.; Livage, J.; Bullot, J. *Philos. Mag. B* **1983**, *47*, 279.

(34) Sega, K.; Kuroda, Y.; Sakata, H. *J. Mater. Sci.* **1998**, *33*, 1303.

(35) Budai, J. D.; Hong, J. W.; Manley, M. E.; Specht, E. D.; Li, C. W.; Tischler, J. Z.; Abernathy, D. L.; Said, A. H.; Leu, B. M.; Boatner, L. A.; McQueeney, R. J.; Delaire, O. *Nature* **2014**, *515*, 535.

(36) Baik, J. M.; Kim, M. H.; Larson, C.; Yavuz, C. T.; Stucky, G. D.; Wodtke, A. M.; Moskovits, M. *Nano Lett.* **2009**, *9*, 3980.

(37) Tamaki, H.; Watanabe, H.; Kamiyama, S.; Oaki, Y.; Imai, H. *Angew. Chem., Int. Ed.* **2014**, *53*, 10706.

(38) (a) Streb, C. *Dalton Trans.* **2012**, *41*, 1651. (b) Tucher, J.; Wu, Y. L.; Nye, L. C.; Ivanovic-Burmazovic, I.; Khusniyarov, M. M.; Streb, C. *Dalton Trans.* **2012**, *41*, 9938.

(39) Tucher, J.; Peuntinger, K.; Margraf, J. T.; Clark, T.; Guldi, D. M.; Streb, C. *Chem. - Eur. J.* **2015**, *21*, 8716.

(40) The accurate absolute rate constant $k_1(Sc_{36}O_{55}^- + n\text{-}C_4H_{10})$ was fitted to be 2.84×10^{-10} cm^3 molecule^{-1} s^{-1} from a pressure-dependent experiment. The k_1^{rel} values of $(Sc_2O_3)_nO^-$ clusters with n = 1−16 were taken from ref 14.

(41) Allred, A. L. *J. Inorg. Nucl. Chem.* **1961**, *17*, 215.

(42) van Hieu, N.; Lichtman, D. *J. Vac. Sci. Technol.* **1981**, *18*, 49.

(43) Emeline, A. V.; Kataeva, G. V.; Ryabchuk, V. K.; Serpone, N. *J. Phys. Chem. B* **1999**, *103*, 9190.

DOI: 10.1021/jacs.6b10839
J. Am. Chem. Soc. 2017, 139, 342−347